I. Troch, F. Breitenecker, eds. ISBN 978-3-901608-35-3

MODEL ORDER REDUCTION FOR SEMI-EXPLICIT SYSTEMS OF DIFFERENTIAL ALGEBRAIC EQUATIONS

Kasra Mohaghegh[1], Roland Pulch[1], Michael Striebel[2], Jan ter Maten[3]
[1]Bergische Universität Wuppertal, Germany, [2]Technische Universität Chemnitz, Germany,
[3]NXP Semiconductors, Netherlands.

Corresponding author: Kasra Mohaghegh
Lehrstuhl für Angewandte Mathematik und Numerische Mathematik
Bergische Universität Wuppertal – D-42119 Wupperal, Gaußstr. 20 – Germany
Email: mohaghegh@math.uni − wuppertal.de

Abstract. Increasing complexity of mathematical models demands techniques of model order reduction (MOR) that enable an efficient numerical simulation. For example, network approaches yield systems of differential algebraic equations (DAEs) in electric circuit simulation. Thereby, miniaturization and increasing packing densities result in extremely large DAE systems. MOR methods are well developed for linear systems of ordinary differential equations (ODEs), whereas the nonlinear case represents still an open field of research. We consider MOR for semi-explicit systems of DAEs. Techniques for ODEs can be generalized to semi-explicit DAEs by a direct or an indirect approach. In the direct approach, we introduce artificial parameters in the system. Accordingly, MOR methods for ODEs can be applied to the regularized system. Numerical simulations using the constructed MOR strategies are presented.

1 Introduction

For large systems of ordinary differential equations (ODEs), efficient model order reduction (MOR) methods already exist in the linear case, see [1]. We want to generalize according techniques to the case of differential algebraic equations (DAEs). On the one hand, a high-index DAE problem can be converted into a lower-index system by analytic differentiations, see [2]. A transformation to index zero yields an equivalent system of ODEs. On the other hand, a regularization is directly feasible in case of semi-explicit systems of DAEs. Thereby, we obtain a singular perturbed problem of ODEs with an artificial parameter. Thus according MOR techniques can be applied to the ODE system. An MOR approach for DAEs is achieved by considering the limit to zero of the artificial parameter.

Systems of DAEs result in the mathematical modeling of a wide variety of problems like electric circuit design, for example. We consider a semi-explicit system

$$\begin{aligned} y'(t) &= f(y(t),z(t)), & y:\mathbb{R}\to\mathbb{R}^k \\ 0 &= g(y(t),z(t)), & z:\mathbb{R}\to\mathbb{R}^l \end{aligned} \tag{1}$$

with differential and perturbation index 1 or 2. For the construction of numerical methods to solve initial value problems of (1), the direct as well as the indirect approach can be used. The direct approach applies an ε-*embedding* of the DAEs (1), i.e., the system changes into

$$\begin{aligned} y'(t) &= f(y(t),z(t)) \\ \varepsilon z'(t) &= g(y(t),z(t)) \end{aligned} \quad \Leftrightarrow \quad \begin{aligned} y'(t) &= f(y(t),z(t)) \\ z'(t) &= \tfrac{1}{\varepsilon} g(y(t),z(t)) \end{aligned} \tag{2}$$

with a real parameter $\varepsilon \neq 0$. Techniques for ODEs can be employed for the singularly perturbed system (2). The limit $\varepsilon \to 0$ yields an approach for solving the DAEs (1). The applicability of the resulting method still has to be investigated.

Alternatively, the indirect approach is based on the *state space form* of the DAEs (1) with index 1, i.e.,

$$y'(t) = f(y(t),\Phi(y(t))) \tag{3}$$

with $z(t) = \Phi(y(t))$. To evaluate the function Φ, the nonlinear system

$$g(y(t),\Phi(y(t))) = 0 \tag{4}$$

is solved for given value $y(t)$. Consequently, the system (3) represents ODEs for the differential variables y and ODE methods can be applied. In each evaluation of the right-hand side in (3), a nonlinear system (4) has to be solved. More details on techniques based on the ε-embedding and the state space form can be found in [7].

Although some MOR methods for DAEs already exist, several techniques are restricted to ODEs or exhibit better properties in the ODE case in comparison to the DAE case. The direct or the indirect approach enables the usage of MOR schemes for ODEs (2) or (3), where an approximation with respect to the original DAEs (1) follows. The aim is to obtain suggestions for MOR schemes via these strategies, where the quality of the resulting approximations still has to be analyzed in each method.

In this work, we focus on the direct approach for semi-explicit system of DAEs, i.e., the ε-embedding is considered. MOR methods are applied to the singularly perturbed system (2). Two scenarios exist to achieve an approximation of the behavior of the original DAEs (1) by MOR. Firstly, an MOR scheme can be applied to the system (2) using a constant $\varepsilon \neq 0$, which is chosen sufficiently small such that a good approximation is obtained. Secondly, a parametric MOR method yields a reduced description of the system of ODEs, where the parameter ε still represents an independent variable. Hence the limit $\varepsilon \to 0$ causes an approach for an approximation of the original DAEs.

We investigate the two approaches with respect to MOR methods based on an approximation of the transfer function, which describes the input-output behavior of the system in frequency domain. We present numerical simulations using two linear semi-explicit systems of DAEs, which follow from mathematical models of electric circuits. Thereby, the two test examples are scalable, i.e., the differential part and/or the algebraic part of the systems can be selected arbitrarily large, whereas the input-output behavior remains the same.

2 Model Order Reduction and ε-Embedding

A continuous time-invariant (lumped) multi-input multi-output linear dynamical system exhibits the form:

$$\left\{ \begin{array}{rcll} C\frac{dx(t)}{dt} & = & -Gx(t)+Bu(t), & x(0)=x_0, \\ w(t) & = & Lx(t)+Du(t), & \end{array} \right. \tag{5}$$

where $x(t) \in \mathbb{R}^n$ is the inner state, $u(t) \in \mathbb{R}^m$ is the input and $w(t) \in \mathbb{R}^p$ is the output. The dimension n of the state vector is called the order of the system. C, G, B, L and D are the state space matrices. The dimension n of the system coincides to the order of elements contained in an electric circuit if applied in circuit simulation.

We restrict to semi-explicit DAE systems of the type (5). According to (1), the solution x and the matrix C exhibit the partitioning:

$$x = \begin{pmatrix} y \\ z \end{pmatrix}, \qquad C = \begin{pmatrix} I_{k\times k} & 0 \\ 0 & 0_{l\times l} \end{pmatrix}. \tag{6}$$

The order of the system is $n = k + l$, where k and l are the dimensions of the differential part and the algebraic part (constraints), respectively, defined in the semi-explicit system (1).

The matrix C in (5) is singular (G is allowed to be singular), and we only assume that the pencil $G+sC$ is *regular*, i.e., the matrix $G+sC$ is singular only for a finite number of values $s \in \mathbb{C}$. Hence initial value problems of (5) exhibit unique solutions provided that the initial values are consistent. For more details on existence and uniqueness of solutions, see [7], where these results are given in Chapter VII.1.

A linear system of the form (5) is often referred to as the representation of the system in the time domain, or in the state space. Equivalently, one can also represent the system in the frequency domain via the Laplace transform. Recall that for a vector-valued function $f(t)$, the Laplace transform is defined by:

$$F(s) := \mathbb{L}\{f(t)\} = \int_0^\infty f(t)e^{-st}\,dt, \qquad s \in \mathbb{C}, \tag{7}$$

which applies the transformation in each component separately. The physically meaningful values of the complex variable s are $s = i\omega$, where $\omega \geq 0$ is referred to as the frequency. Taking the Laplace transformation of the system (5), we obtain the following frequency domain formulation of the system (without loss

of generality we assume that $D = 0$):

$$\left\{ \begin{array}{rcl} sCX(s) & = & -GX(s)+BU(s), \\ W(s) & = & LX(s), \end{array} \right. \tag{8}$$

where $X(s)$, $U(s)$ and $W(s)$ represent the Laplace transforms of $x(t)$, $u(t)$ and $w(t)$, respectively. Eliminating the variable $X(s)$ in (8), we recognize that the input $U(s)$ and the output $W(s)$ in the frequency domain are related by the following $p \times m$ matrix-valued rational function:

$$H(s) = L \cdot (G+sC)^{-1} \cdot B = L \cdot (G+s \begin{pmatrix} I_{k\times k} & 0 \\ 0 & 0_{l\times l} \end{pmatrix})^{-1} \cdot B \tag{9}$$

provided that $\det(G+sC) \neq 0$. The mapping $H(s)$ from (9) is known as the *transfer function* or *Laplace-domain impulse response* of the linear system (5). Following the direct approach, the ε-embedding changes the system (5) to:

$$\left\{ \begin{array}{rcll} C(\varepsilon)\frac{dx(t)}{dt} & = & -Gx(t)+Bu(t), & x(0) = x_0, \\ w(t) & = & Lx(t), & \end{array} \right. \tag{10}$$

where

$$C(\varepsilon) = \begin{pmatrix} I_{k\times k} & 0 \\ 0 & \varepsilon I_{l\times l} \end{pmatrix} \qquad \text{for } \varepsilon \in \mathbb{R}$$

with the same inner state and input/output as before. For $\varepsilon \neq 0$, the matrix C is regular in (10) and the transfer function reads:

$$H_\varepsilon(s) = L \cdot (G+s \cdot C(\varepsilon))^{-1} \cdot B \tag{11}$$

provided that $\det(G+sC(\varepsilon)) \neq 0$. For convenience, we introduce the notation

$$M(s,\varepsilon) := sC(\varepsilon) = s \begin{pmatrix} I_{k\times k} & 0 \\ 0 & \varepsilon I_{l\times l} \end{pmatrix}. \tag{12}$$

It holds $M(s,0) = sC$ with C from (5).

Concerning the relation between the original system (5) and the regularized system (10) with respect to the transfer function, we achieve the following statement. Without loss of generality, the induced matrix norm of the Euclidean vector norm is applied.

Theorem 1. *For fixed $s \in \mathbb{C}$ with $\det(G+M(s,0)) \neq 0$ and $\varepsilon \in \mathbb{R}$ satisfying*

$$|\varepsilon| \leq \frac{c}{\|(G+M(s,0))^{-1}\|_2} \tag{13}$$

for some $c \in (0,1)$, the transfer functions $H(s)$ and $H_\varepsilon(s)$ exist and it holds

$$\|H(s)-H_\varepsilon(s)\|_2 \leq \|L\|_2 \cdot \|B\|_2 \cdot K(s) \cdot |s| \cdot |\varepsilon|$$

with the constant

$$K(s) = \frac{1}{1-c} \left\|(G+M(s,0))^{-1}\right\|_2^2.$$

Proof. The condition (13) guarantees that the matrices $G+M(s,\varepsilon)$ are regular. The definition of the transfer functions implies:

$$\|H(s)-H_\varepsilon(s)\|_2 \leq \|L\|_2 \cdot \left\|(G+M(s,0))^{-1}-(G+M(s,\varepsilon))^{-1}\right\|_2 \cdot \|B\|_2 .$$

Using basic calculations, the mid term in right-hand side of the expression above becomes:

$$\begin{array}{rcl} \left\|(G+M(s,0))^{-1}-(G+M(s,\varepsilon))^{-1}\right\|_2 & \leq & \frac{1}{1-c}\left\|(G+M(s,0))^{-1}\right\|_2^2 \cdot \|M(s,0)-M(s,\varepsilon)\|_2 \\ & = & K(s)\,\|M(s,0)-M(s,\varepsilon)\|_2 . \end{array}$$

Due to the definition (12), we obtain:

$$\|M(s,0)-M(\varepsilon,s)\|_2 = |s|\cdot\left\|\begin{pmatrix} 0 & 0 \\ 0 & \varepsilon I_{l\times l}\end{pmatrix}\right\|_2 = |s|\cdot|\varepsilon|\,.$$

Thus the proof is completed. □

We conclude from Theorem 1 that

$$\lim_{\varepsilon\to 0} H_\varepsilon(s) = H(s) \tag{14}$$

for each $s\in\mathbb{C}$ with $G+sC$ regular. For $s\in\mathbb{R}$, we also obtain the uniform convergence

$$\|H(s)-H_\varepsilon(s)\|_2 \le \hat{K}\,|\varepsilon| \quad \text{for all } s\in S$$

in a compact domain $S\subset\mathbb{C}$ with the constant

$$\hat{K} = \frac{\|L\|_2\cdot\|B\|_2}{1-c}\max_{s\in S}\left\|(G+M(s,0))^{-1}\right\|_2^2\cdot|s|$$

provided that $\det(G+M(s,0))\neq 0$ holds for all $s\in S$. In particular, compact subsets S of the real or imaginary axis can be considered.

Furthermore, Theorem 1 implies the property

$$\lim_{s\to 0} H(s)-H_\varepsilon(s) = 0$$

for fixed ε assuming $\det G\neq 0$. However, we are not interested in the limit case of small variables s.

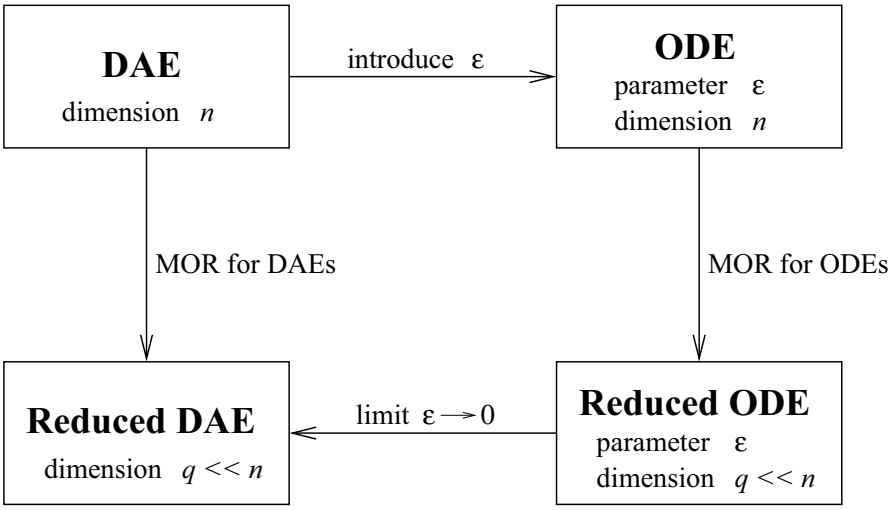

Figure 1: The approach of the ε-embedding for MOR.

For MOR of the DAE system (5), we have two ways to handle the artificial parameter ε, which results in two different scenarios. In the first scenario, we fix a small value of the parameter ε. Thus we use one of the standard techniques for the reduction of the corresponding ODE system. Finally, we achieve a reduced ODE (with small ε inside). The ODE system with small ε represents a regularized DAE. Any reduction scheme for ODEs is feasible. Recent research shows that the Poor Man's TBR (PMTBR), see [8], can be applied efficiently if the matrix C in (5) is regular, which is indeed our case. The test case with the simulation result will be presented in the following section. In the second scenario, the parameter ε is considered as an independent variable (value not predetermined). We can use the parametric MOR for reducing the corresponding ODE system. The applied parametric MOR is based on [3, 4] in this case. The

limit $\varepsilon \to 0$ yields the results in an approximation of original DAEs (5). The existence of the approximation in this limit still has to be analyzed. Figure 1 illustrates the strategy.

Theorem 1 provides the theoretical background for the first scenario. We apply an MOR scheme based on an approximation of the transfer function to the system of ODEs (10). Let $\tilde{H}_\varepsilon(s)$ be a corresponding approximation of $H_\varepsilon(s)$. It follows

$$\|H(s) - \tilde{H}_\varepsilon(s)\|_2 \leq \|H(s) - H_\varepsilon(s)\|_2 + \|H_\varepsilon(s) - \tilde{H}_\varepsilon(s)\|_2$$

for each $s \in \mathbb{C}$ with $\det(G+sC) \neq 0$. Due to Theorem 1, the first term becomes small for sufficiently small parameter ε. However, ε should not be chosen smaller than the machine precision on a computer. The second term depends on the applicability of an efficient MOR method to the ODEs (10). Thus $\tilde{H}_\varepsilon(s)$ can be seen as an approximation of the transfer function $H(s)$ belonging to the system of DAEs (5).

3 Test Example

We investigate a linear forced LC-oscillator with a capacitor, a resistor and an inductor in series. As we want to extend this LC-oscillator to a scalable benchmark problem (both in differential part and algebraic part), we arrange n resistors in parallel and m capacitors in series, see Figure 2 (left). A kind of sparse tableau modeling, cf. [6], has been studied for this case, where the currents through the resistors are defined as unknowns. If we apply the modified nodal analysis (MNA) [5] to this case, then the equations of the constraints are not scalable any more. Consequently, we arrange the n resistors in series instead, see Figure 2 (right). Then the charge oriented MNA is studied. The values for capacitors and resistors (in both cases) are defined such that the total capacitance and the total resistance coincides for each n and m. Moreover, all capacitances and resistances are chosen with the same parameters C and R, respectively. The LC-oscillator is forced by an input signal, since a current source

$$u(t) = I_0 \sin\left(\frac{2\pi}{T}t\right)$$

with fixed amplitude $I_0 > 0$ and period $T > 0$ is added to node 1 in both cases.

Example 1. In the case of resistors in parallel, the state variables $x \in \mathbb{R}^{m+n+3}$ consist of the voltages e of the nodes, the current i_L traversing the inductor, the currents i_R running through the resistors R_i and the current i_I from the external source. The used physical parameters are

$$L = 10^{-6}\ \text{H}, \qquad R = n10^4\ \Omega, \qquad C = m10^{-9}\ \text{F},$$

where $n = 300$ and $m = 300$ represent the numbers of the resistors and capacitors, respectively.

The matrix notation of the sparse tableau analysis reads:

$$\begin{bmatrix} A_C C A_C^\top & 0 & 0 & 0 \\ 0 & L & 0 & 0 \\ 0 & 0 & 0 & 0 \\ 0 & 0 & 0 & 0 \end{bmatrix} \frac{d}{dt} \begin{bmatrix} e \\ i_L \\ i_R \\ i_I \end{bmatrix} + \begin{bmatrix} 0 & A_L & A_R & A_I \\ -A_L^\top & 0 & 0 & 0 \\ -GA_R^\top & 0 & I_{n\times n} & 0 \\ 0 & 0 & 0 & 1 \end{bmatrix} \begin{bmatrix} e \\ i_L \\ i_R \\ i_I \end{bmatrix} + \begin{bmatrix} 0 \\ 0 \\ 0 \\ -1 \end{bmatrix} u(t) = 0.$$

Example 2. In the case of resistors in series, the state variables $x \in \mathbb{R}^{2m+n+3}$ include the voltages e of the nodes, charges q and a flux ϕ, the current i_L traversing the inductor and the current i_I from the external source. The physical parameters are chosen as

$$L = 10^{-6}\ \text{H}, \qquad R = \tfrac{1}{n}10^4\ \Omega, \qquad C = m10^{-9}\ \text{F},$$

where $n = 200$ and $m = 200$ indicate again the numbers of the resistors and capacitors, respectively.

The matrix notation of the charge oriented MNA becomes:

$$\begin{bmatrix} A_C & 0 & 0 & 0 & 0 \\ 0 & 1 & 0 & 0 & 0 \\ 0 & 0 & 0 & 0 & 0 \\ 0 & 0 & 0 & 0 & 0 \\ 0 & 0 & 0 & 0 & 0 \end{bmatrix} \frac{d}{dt} \begin{bmatrix} q \\ \phi \\ e \\ i_L \\ i_I \end{bmatrix} + \begin{bmatrix} 0 & 0 & A_R G A_R^\top & A_L & A_I \\ 0 & 0 & -A_L^\top & 0 & 0 \\ I_{m\times m} & 0 & -CA_C^\top & 0 & 0 \\ 0 & 1 & 0 & -L & 0 \\ 0 & 0 & 0 & 0 & 1 \end{bmatrix} \begin{bmatrix} q \\ \phi \\ e \\ i_L \\ i_I \end{bmatrix} + \begin{bmatrix} 0 \\ 0 \\ 0 \\ 0 \\ -1 \end{bmatrix} u(t) = 0.$$

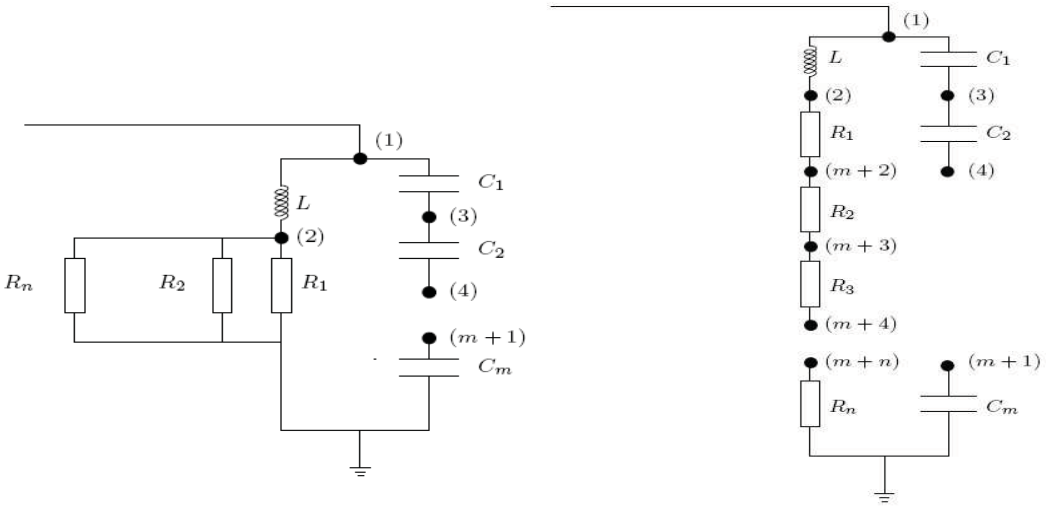

Figure 2: Left: RLC circuit example 1, Right: RLC circuit example 2.

4 Simulation Results

We apply the test examples from the previous section considering the first scenario. For the simulation of Example 1, we arrange the constant parameter $\varepsilon = 10^{-12}$. The PMTBR yields the reduction of the corresponding ODE system. Figure 3 shows the transfer function both for the DAE, the ODE and the reduced ODE with fixed ε. The numbers in the parentheses indicate the order of the systems. A Bode magnitude (phase) plot of a transfer function plots the magnitude (phase) of $H(i\omega)$, usually in decibel, for a number of frequencies ω in the frequency range of interest, see Figures 3, 5 and 7.

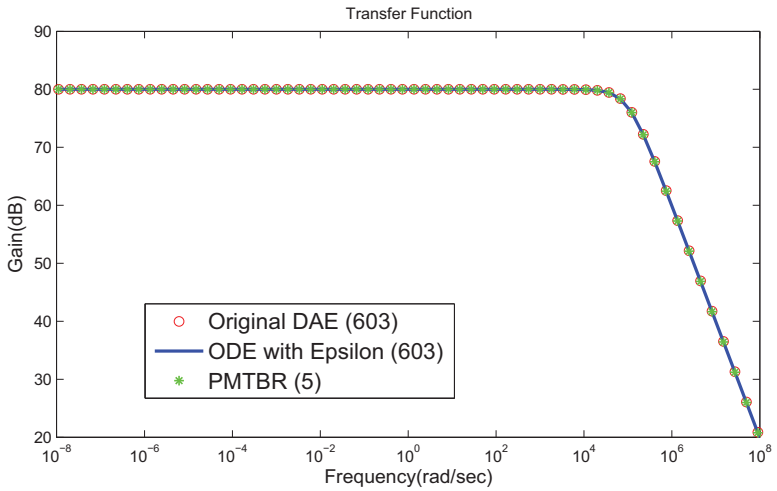

Figure 3: Transfer functions for original DAE and ODE and reduced transfer function, Example 1.

In Figure 4, the dashed line illustrates the absolute error between the DAE system and the ODE system. The two systems exhibit a good agreement for low frequencies and the error increases just for higher frequencies and then smoothly decreasing for still higher frequencies. The solid line in Figure 4 describes the absolute error between the original DAE system and the reduced ODE with fixed ε.

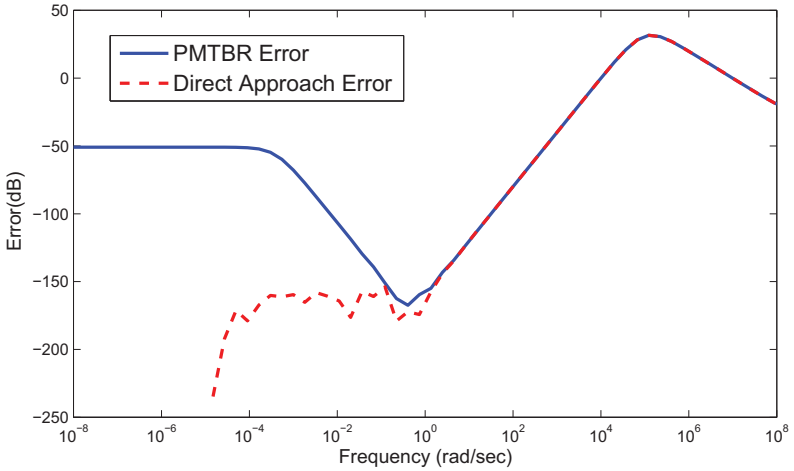

Figure 4: Corresponding error plot, Example 1.

For the simulation of Example 2, we choose the constant parameter $\varepsilon = 10^{-15}$. Again the PMTBR is used as a reduction scheme for the ODE system. Figure 5 depicts the transfer function both for the DAE and the ODE and the reduced ODE with fixed ε. This simulation is more sensitive with respect to ε than the previous example. This sensitivity forced us to arrange a smaller regularization parameter ε in this case.

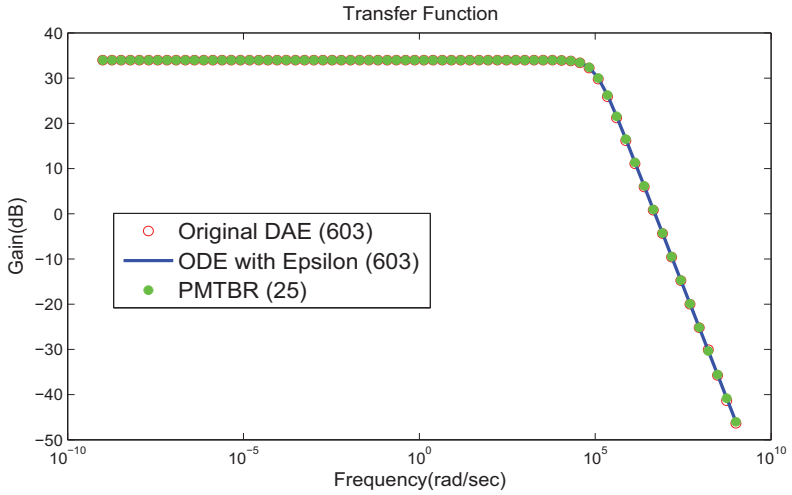

Figure 5: Transfer functions for original DAE and ODE and reduced transfer function, Example 2.

The absolute error of the approaches is shown in Figure 6. The results corresponding to the DAE system and the ODE system demonstrate the same qualitative behavior as in Example 1. The error of the regularization and the error including the regularization as well as the reduction coincide for high frequencies.

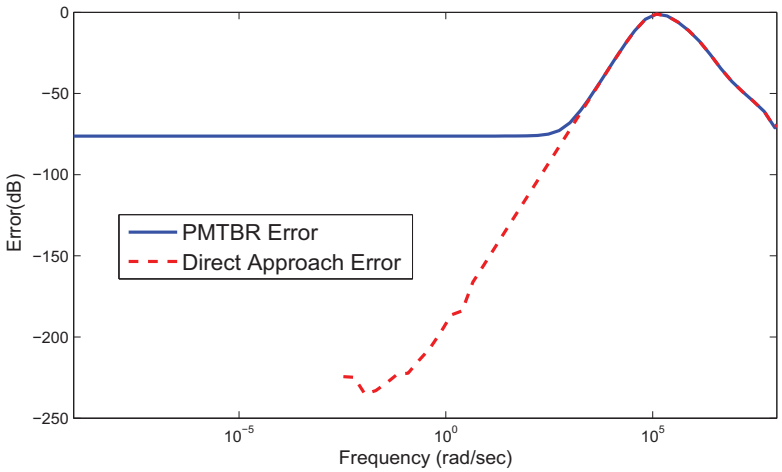

Figure 6: Corresponding error plot, Example 1.

The underlying electric circuits represent benchmarks, since they are designed such that MOR methods can be applied efficiently. Hence the PMTBR scheme produces reliable results in the test examples, although the PMTBR is not an efficient reduction scheme for DAEs in general.

The second scenario with parametric MOR is studied now, see [4] for more details. Thereby, we apply the systems of Example 1 only. The limit $\varepsilon \to 0$ yields the desired result for the DAEs, see Figure 7. The same order as in the first scenario causes a too large computational effort so we choose the order of the system smaller in this case as the parameter ε has to be considered during the reduction. The error of this parametric reduction scheme is shown in Figure 8. The error plot illustrates a good agreement of the transfer functions for high frequencies. Although the error increases for low frequencies, the difference remains bounded.

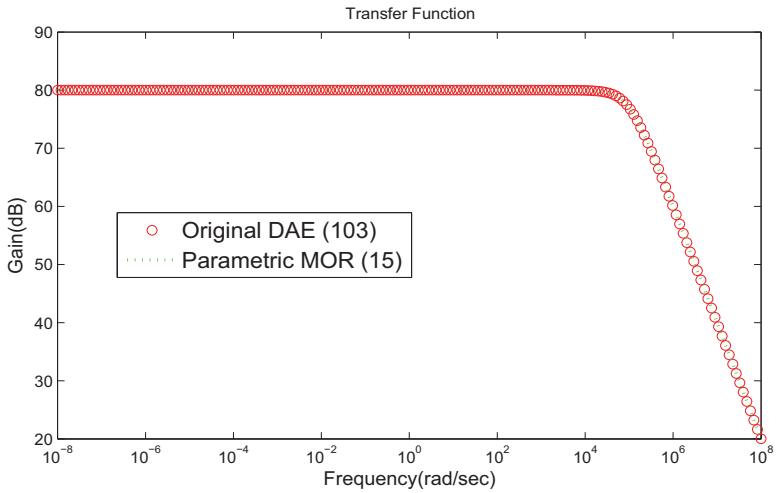

Figure 7: Transfer function for original DAE and parametric MOR with $\varepsilon \to 0$, Example 1.

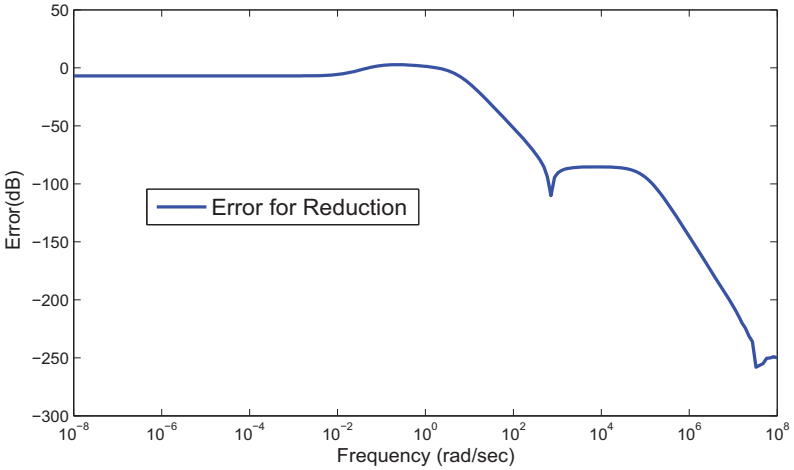

Figure 8: Corresponding error plot for parametric MOR with $\varepsilon \to 0$, Example 1.

5 Conclusions

The ε-embedding transforms a semi-explicit system of DAEs into a singularly perturbed system of ODEs. MOR methods for ODEs can be applied to the constructed system, where the parameter ε is included. The input-output behavior of both DAE system and ODE system is described by respective transfer functions in frequency domain. We have shown that the transfer function of the singularly perturbed system of ODEs converges to the transfer function of the original DAEs in the limit of a vanishing parameter ε. MOR techniques can be applied within two scenarios: fixing a small ε or performing the limit $\varepsilon \to 0$ in a parametric MOR. We have presented numerical simulations, which produce good approximations using the two approaches in case of linear test examples. As both scenarios are sensitive with respect to the parameter ε, this sensitivity should be discussed further. Moreover, simulation in time domain will be part of future work.

Acknowledgments.

The work presented is supported by the EU Marie Curie Research-Training-Network COMSON (COupled Multiscale Simulation and Optimization in Nanoelectronics) and the EU Marie Curie Transfer-of-Knowledge project O-MOORE-NICE! (Operational MOdel Order REduction for Nanoscale IC Electronics).

6 References

[1] A.C. Antoulas: *Approximation of large-scale Dynamical Systems, advances in design and control*. SIAM, 2005.

[2] U.M. Ascher, and L.R. Petzold: *Computer Methods for Ordinary Differential Equations and Differential-Algebraic Equations*. SIAM, 1998.

[3] L. Daniel, O. Siong, L. Chay, K. Lee, and J. White: *A multiparameter Moment Matching Model reduction Approach for Geometrically Parameterized Interconnect Performance Models*. IEEE Trans. Comput.-Aided Des. Integr. Circuits Syst., 22-5 (2004), 678-693.

[4] L. Feng, and P. Benner: *A Robust Algorithm for Parametric Model Order Reduction based on Implicit Moment Matching*. Proceedings in Applied Mathematics and Mechanics, Oct. 2007.

[5] M. Günther, and U. Feldmann: *CAD based electric circuit modeling in industry I: mathematical structure and index of network equations.* Surv. Math. Ind., 8 (1999), 97-129.

[6] G.D. Hachtel, R.K. Brayton, and F.G. Gustavson: *The sparse tableau approach to network analysis and design.* IEEE Trans. Circ. Theory, 18 (1971), 101-113.

[7] E. Hairer, and G. Wanner: *Solving Ordinary Differential Equations II: Stiff and Differential-Algebraic Problems*. (2nd Ed.) Springer, Berlin 2002.

[8] J. Phillips, and L.M. Silveira: *Poor man's TBR: a simple model reduction scheme*. Proceedings of the Design, Automation and Test in Europe Conference and Exhibition (DATE), Vol. 2 (2004), 938-943.